Exceptional points in coupled dissipative dynamical systems

Jung-Wan Ryu,[1] Woo-Sik Son,[2] Dong-Uk Hwang,[2] Soo-Young Lee,[1] and Sang Wook Kim[3,*]
[1]*School of Electronics Engineering, Kyungpook National University, Daegu 702-701, Korea*
[2]*National Institute for Mathematical Sciences, Daejeon 305-811, South Korea*
[3]*Department of Physics Education, Pusan National University, Busan 609-735, South Korea*
(Received 11 February 2015; published 13 May 2015)

We study the transient behavior in coupled dissipative dynamical systems based on the linear analysis around the steady state. We find that the transient time is minimized at a specific set of system parameters and show that at this parameter set, two eigenvalues and two eigenvectors of the Jacobian matrix coalesce at the same time; this degenerate point is called the exceptional point. For the case of coupled limit-cycle oscillators, we investigate the transient behavior into the amplitude death state, and clarify that the exceptional point is associated with a critical point of frequency locking, as well as the transition of the envelope oscillation.

DOI: 10.1103/PhysRevE.91.052910 PACS number(s): 05.45.Xt, 02.10.Ud

I. INTRODUCTION

In the eigenvalue problem of a non-Hermitian matrix, an exceptional point (EP) is a square-root branch point on a two-dimensional parameter space, at which not only eigenvalues but also the associated eigenvectors coalesce [1,2]. The peculiar feature related to the EP is the exchange of eigenvalues and eigenvectors after a parameter variation encircling the EP once, of which the topological structure is the same as that of a Möbius strip [3]. The EPs and relating interesting phenomena have mainly been studied in open quantum systems described by non-Hermitian Hamiltonians, such as atomic spectra in fields [4,5], microwave cavity experiments [6,7], chaotic optical microcavities [8], *PT*-symmetric quantum systems [9–11], and so on. Besides the open quantum systems, the EPs are also observed in coupled driven damped oscillators realized by electric circuits, which are purely classical systems [12,13].

The amplitude death (AD) is the complete suppression of oscillations of the entire system when the nonlinear dynamical systems are coupled [14]. The AD has been observed in many coupled dynamical systems and the AD is achieved by various types of coupling interactions, i.e., the diffusive coupling in mismatched oscillators [15–18], delayed coupling [19–23], conjugate coupling [24], dynamical coupling [25], nonlinear coupling [26,27], etc. The AD has also been studied in networks of coupled oscillators [17,28] and a variety of topologies such as a ring [29,30], small world [31], and scale-free networks [32]. Recently, the suppressions of oscillations are strictly classified into amplitude death and oscillation death, where the asymptotic steady state is homogeneous and inhomogeneous, respectively [14,33].

In this paper, we study the transient behaviors of coupled dissipative dynamical systems based on the linear analysis around the steady state. We find that the systems show the largest damping rate at an EP, which comes from the intrinsic feature of a square-root branch point. For the case of coupled limit-cycle oscillators, the transient behavior into the amplitude death state is studied. We demonstrate that the EP is associated with a critical point of frequency locking, as well as the transition of the envelope oscillation.

This paper is organized as follows. In Sec. II, we show the occurrence of EP in coupled damped oscillators and discuss the damping behavior around the EP in a pedagogical way. In Sec. III, we present the transient behavior into the AD in coupled limit-cycle oscillators, and it is explained based on the existence of an EP. Finally, we summarize our results in Sec. IV.

II. EXCEPTIONAL POINT IN COUPLED DAMPED OSCILLATORS

We consider the coupled damped oscillators,

$$\begin{aligned} \ddot{x}_1 + \gamma_1 \dot{x}_1 + \omega_1^2 x_1 &= -k x_2, \\ \ddot{x}_2 + \gamma_2 \dot{x}_2 + \omega_2^2 x_2 &= -k x_1, \end{aligned} \tag{1}$$

where γ_i and ω_i $(i = 1,2)$ are the damping ratio and undamped angular frequency of the ith oscillator, and k is the coupling constant. Figure 1 shows the time series of x_1 and x_2 of Eq. (1) in the logarithmic scale when $\omega_1 = \omega_2 = 1.0$ and $\gamma_1 = 0$. First, we consider the uncoupled case, $k = 0$. As we set $\gamma_1 = 0$ and $\gamma_2 = 0.1$, the time series of x_1 exhibits a stationary oscillation without damping, while an exponential damping appears in the time series of x_2, as shown in Fig. 1(a). Next, we consider a finite coupling strength of $k = 0.1$. In Fig. 1(b) with $\gamma_1 = 0$ and $\gamma_2 = 0.1$, both time series of x_1 and x_2 exhibit decays with envelope oscillations. Their decay rates, given by the slope of time series of x_1 and x_2 in the logarithmic plot, are equal. As γ_2 increases from 0.1, the period of the envelope oscillation and the decay rate increase. At $\gamma_2 \sim 0.2$, the envelope oscillation disappears and the decay rate reaches a maximum [see Fig. 1(c)]. When γ_2 increases further, the decay rate decreases again. For example, the time series of the case with $\gamma_2 = 0.3$ is shown in Fig. 1(d). Although the amplitudes of two oscillators are different, as shown in the inset, their decay rates are equal. In our work, we concentrate on the case where each uncoupled oscillator has a zero or weak damping ratio so that their dampings are underdamped.

In order to understand the variation of decay rate with γ_2 and its maximum at $\gamma_2 \sim 0.2$, we analyze the eigenvalues of a stability matrix around the origin. Equation (1) can be rewritten as

$$\begin{aligned} \dot{x}_1 &= y_1, \quad \dot{y}_1 = -\gamma_1 y_1 - \omega_1^2 x_1 - k x_2, \\ \dot{x}_2 &= y_2, \quad \dot{y}_2 = -\gamma_2 y_2 - \omega_2^2 x_2 - k x_1. \end{aligned} \tag{2}$$

*swkim0412@pusan.ac.kr

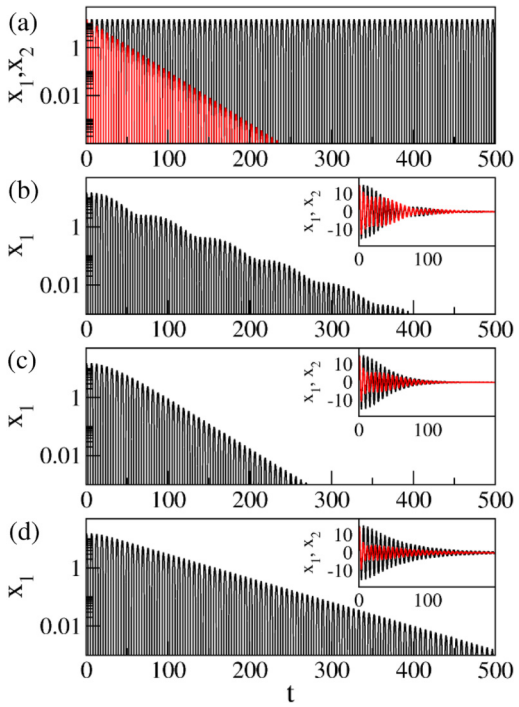

FIG. 1. (Color online) Time series of x_1 (black) and x_2 (red) when $\omega_1 = \omega_2 = 1.0$ and $\gamma_1 = 0.0$. (a) No coupling case of $k = 0.0$ with $\gamma_2 = 0.1$. Coupling cases of $k = 0.1$ with (b) $\gamma_2 = 0.1$, (c) $\gamma_2 = 0.2$, and (d) $\gamma_2 = 0.3$. The insets show linearly scaled time series.

This set of equations is represented by a vector equation, $\dot{\vec{z}}(t) = M\vec{z}(t)$, where $\vec{z}(t) = [x_1(t), y_1(t), x_2(t), y_2(t)]^T$. The stability matrix M is then given by

$$M = \begin{pmatrix} 0 & 1 & 0 & 0 \\ -\omega_1^2 & -\gamma_1 & -k & 0 \\ 0 & 0 & 0 & 1 \\ -k & 0 & -\omega_2^2 & -\gamma_2 \end{pmatrix}. \quad (3)$$

The eigenvalues λ_l of M are complex numbers, because the matrix M is non-Hermitian. Since the time evolution of an eigenvector $\hat{e}_l$ is given as $e_l(t) = \hat{e}_l \exp(\lambda_l t)$, the real and imaginary parts of the eigenvalues correspond to the decay rates and the angular frequency of the corresponding time series, respectively.

The complex eigenvalues with positive imaginary parts are shown as a function of γ_2 in Figs. 2(a) and 2(b). When $\gamma_2 < 0.2$, the real parts of the two eigenvalues are very close but their imaginary parts are quite different, which means that the dynamics of the eigenvectors would show almost the same decay rate and different angular frequencies. In this range, the time series of x_1 and x_2 would show a constant overall slope given by the close real parts, but they would have an oscillatory envelope whose frequency is determined by the difference of the imaginary parts of eigenvalues. This behavior has been shown in Fig. 1(b). As γ_2 approaches a value of 0.2, the real parts of two eigenvalues decrease and the imaginary parts become closer to each other, which corresponds to the time series with a faster decay and a longer period of envelope oscillation, respectively.

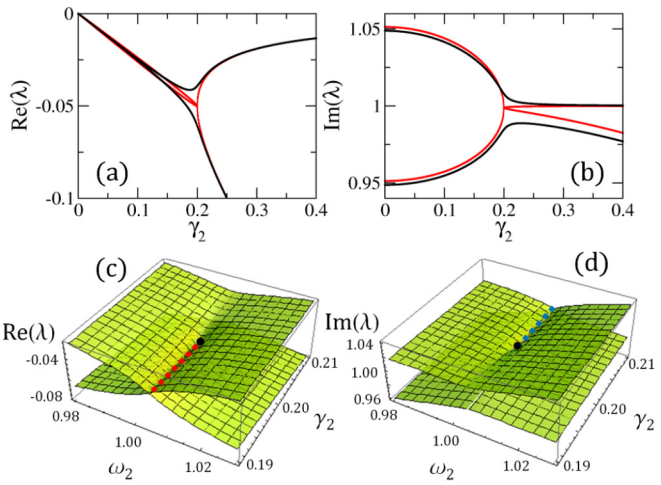

FIG. 2. (Color online) (a) Real and (b) imaginary parts of two eigenvalues of which the imaginary parts are positive as a function of γ_2 when $\omega_2 = 1.0$ (black) and $\omega_2 = 1.005$ (red) with $\gamma_1 = 0.0$ and $\omega_1 = 1.0$. (c) Real and (d) imaginary parts of the eigenvalues near EP as functions of ω_2 and γ_2 when $\omega_1 = 1.0$ and $\gamma_1 = 0.0$. The black circle, red dotted line, and blue dotted line represent the EP, real value crossing line, and imaginary value crossing line, respectively.

As γ_2 goes further beyond 0.2, two real parts start to split but the difference of the two imaginary parts become small. The splitting of two real parts indicates that the time series can be characterized by a combination of fast and slow decays. The fast decay might be seen only in the short-time behavior, and the slow decay, corresponding to the larger real part, dominates the long-time behavior of the time series. Thus, although two imaginary parts are still different, there is no envelope oscillation due to the fast suppression of one eigencomponent with the lower real part [see Fig. 1(d)]. Note that the larger real part, governing long-time behavior, has a minimum value around at $\gamma_2 \sim 0.2$, which explains the maximum decay rate observed in Fig. 1(c).

Note that two complex eigenvalues are very close at $\gamma_2 \sim 0.2$, as shown by the black lines in Figs. 2(a) and 2(b). We can expect that there should be a degenerate point, called the exceptional point (EP) [1,2], where two complex eigenvalues coalesce, in the system parameter space. By slightly adjusting ω_2 as $\omega_2 = 1.005$, we find an EP at $(\omega_2, \gamma_2) \sim (1.005, 0.2)$, which is shown by the red lines in Figs. 2(a) and 2(b). It is well known that two eigenvectors also coalesce at the EP and mathematically the EP is the square-root branch point. The EP can be characterized by a peculiar eigenvalue surfaces in a parameter plane. In Figs. 2(c) and 2(d), the surfaces of the two eigenvalues are plotted in the (ω_2, γ_2) plane. The topology of the surface explains the exchange of two eigenvalues for a parameter variation encircling the EP [3]. It is emphasized that the larger real part becomes a local minimum at the EP, indicating the local maximum decay rate in the parameter plane.

III. EXCEPTIONAL POINT AND AMPLITUDE DEATH IN COUPLED LIMIT-CYCLE OSCILLATORS

In this section, we study the role of the EP when the amplitude death (AD) occurs in coupled limit-cycle oscillators.

Let us start with the following system of two Stuart-Landau limit-cycle oscillators with diffusive coupling,

$$\begin{aligned}\dot{z}_1 &= (R_1 + i\omega_1 - |z_1|^2)z_1 + k(z_2 - z_1),\\ \dot{z}_2 &= (R_2 + i\omega_2 - |z_2|^2)z_2 + k(z_1 - z_2),\end{aligned} \tag{4}$$

where z_j are complex variables, ω_j are the intrinsic angular frequencies of uncoupled jth limit-cycle oscillators, and k is the coupling strength. Without coupling ($k = 0$), two limit-cycle oscillators are attracted to the limit cycle with radii $\sqrt{R_j}$ for $R_j > 0$ and the origin for $R_j < 0$. The Stuart-Landau limit-cycle oscillator is renowned as a paradigmatic model for studying the AD in coupled nonlinear oscillators because it is a prototypical system exhibiting a Hopf bifurcation that can reveal universal features of many practical systems. For instance, a variety of spatiotemporal periodic patterns can be created in two-dimensional lattice of delay-coupled Stuart-Landau oscillators [34].

A. The amplitude death in coupled limit-cycle oscillators

It has been well known that the AD occurs in coupled limit-cycle oscillators at proper k if the $\Delta\omega = \omega_2 - \omega_1$ is sufficiently large when $R_1 = R_2 = 1.0$ [16–18]. In order to obtain the AD region in the parameter space $(\Delta\omega,k)$, we calculate the Jacobian matrix J at the origin, which is given by

$$J = \begin{pmatrix} R_1 - k & -\omega_1 & k & 0 \\ \omega_1 & R_1 - k & 0 & k \\ k & 0 & R_2 - k & -\omega_2 \\ 0 & k & \omega_2 & R_2 - k \end{pmatrix}. \tag{5}$$

The eigenvalues λ of J are complex numbers because the Jacobian matrix J is a non-Hermitian matrix. That is, the real and imaginary parts are the decay (or growing) rates and the angular frequency of the orbit near the origin, respectively.

The occurrence of AD is determined by the stability of the origin, which is related to the maximal value of the real parts of complex eigenvalues. If the maximal value is negative, the origin is a stable fixed point and therefore the system exhibits the AD. The colored region in Figs. 3(a)–3(c) where the maximal value is negative represents the AD regions when $R_2 = 1.0$, 0.0, and -1.0, respectively, with $R_1 = 1.0$. As R_2 decreases from 1.0 to -1.0, the AD region becomes larger. Figure 3(d) clearly shows the transition between positive and negative values of the maximal real parts as a function of k when $\Delta\omega$ is fixed.

B. The exceptional point in coupled limit-cycle oscillators

Similarly as for the case of coupled damped oscillators, there also exists an EP in the coupled limit-cycle oscillators. The EP occurs at $k = 2.0$ when $\Delta\omega = 4.0$ and $R_1 = R_2 = 1.0$, which is the double root position in Figs. 3(d) and 3(e). Considering $R_1 = R_2 = R$, four eigenvalues of Eq. (5) are given by

$$\begin{aligned}&-k + R \pm \sqrt{-\frac{(\Delta\omega)^2}{2} + k^2 - \triangle},\\ &-k + R \pm \sqrt{-\frac{(\Delta\omega)^2}{2} + k^2 + \square},\end{aligned} \tag{6}$$

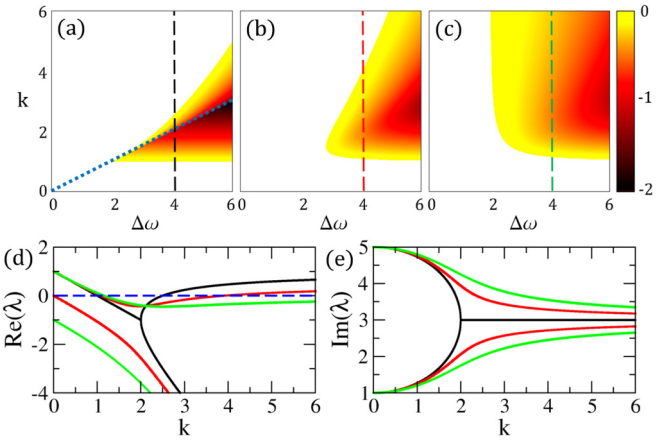

FIG. 3. (Color online) Maximal values of the real parts of eigenvalues with (a) $R_2 = 1.0$, (b) $R_2 = 0.0$, and (c) $R_2 = -1.0$ when $R_1 = 1.0$. The colored and white regions represent negative and positive values, respectively. The blue dotted line represents the EP. (d) Real and (e) imaginary parts of two eigenvalues of which imaginary parts are positive as a function of k when $\Delta\omega = 4.0$ and $R_1 = 1.0$. Black, red, and green curves represent the cases of $R_2 = 1.0$, 0.0, and -1.0, respectively.

where $\triangle = \frac{\Delta\omega}{2}(\sqrt{\Delta\omega^2 - 4k^2} + 2\omega_1) + \omega_1(\sqrt{\Delta\omega^2 - 4k^2} + \omega_1)$ and $\square = \frac{\Delta\omega}{2}(\sqrt{\Delta\omega^2 - 4k^2} - 2\omega_1) + \omega_1(\sqrt{\Delta\omega^2 - 4k^2} - \omega_1)$, respectively. From the condition for EP, i.e., $\triangle = -\square$, the analytic condition for the existence of EP is given by

$$R_1 = R_2, \quad k = \Delta\omega/2. \tag{7}$$

The eigenvectors also coalesce at this condition. According to the Eq. (7), the EP occurs on the line in the parameter space $(\Delta\omega,k)$ when $\Delta R = R_2 - R_1 = 0.0$, as shown in Fig. 3(a). If $\Delta\omega$ is fixed, it is expected that a system shows the fastest attracting to the AD state on the condition of EP, $k = \Delta\omega/2$. Because the decaying rate to the AD state can be considered as a maximal value of Re(λ) and the maximal value of Re(λ) has its minimum at the condition of EP, $k = \Delta\omega/2$ [cf. Fig. 3(d)]. In addition, there is a transition of transient behavior to the AD state on the EP, which is the transition between decaying with envelope oscillation due to the effective beat note for $k < \Delta\omega/2$ and decaying without envelope oscillation for $k > \Delta\omega/2$. It is noted that as R_2 decreases from 1.0, the AD region becomes larger, while the fastest attracting to the AD state occurs on the EP when $R_2 = 1.0$.

Figure 4 shows the complex eigenvalues near the EP in the parameter space $(\Delta R,k)$, which is the singular point.

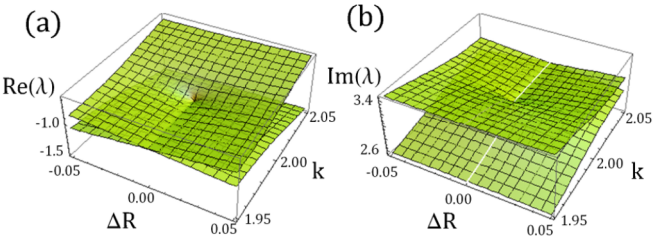

FIG. 4. (Color online) (a) Real and (b) imaginary parts of two eigenvalues near the EP at $(\Delta R,k) = (0.0,2.0)$ when $\Delta\omega = 4.0$

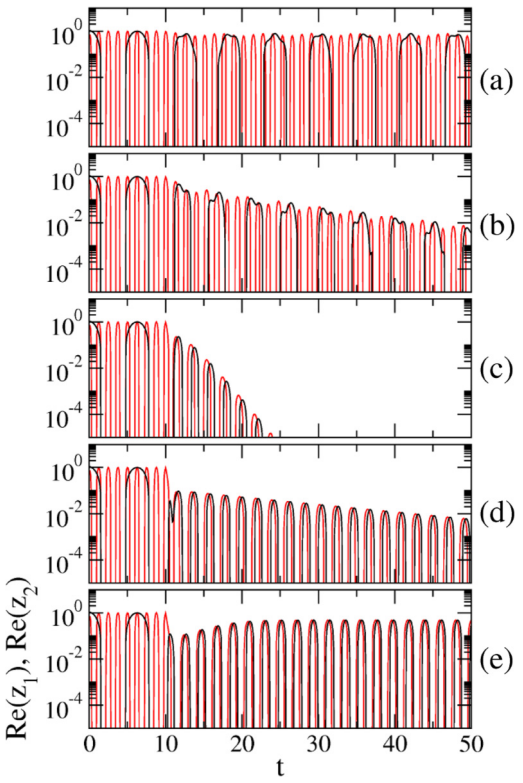

FIG. 5. (Color online) Time series of real parts of z_1 (black) and z_2 (red) with (a) $k = 0.5$, (b) 1.1, (c) 2.0, (d) 2.4, and (e) 3.0 when $\Delta\omega = 4.0$ and $R_1 = R_2 = 1.0$.

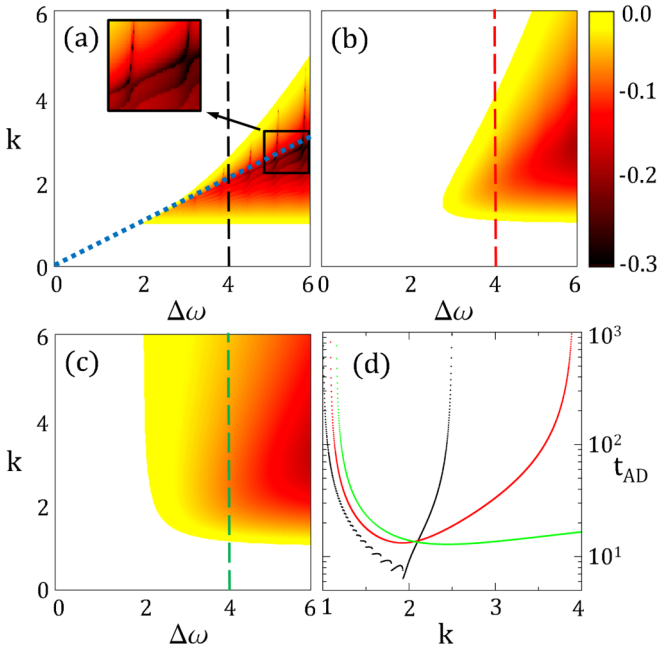

FIG. 6. (Color online) $-(1/t_{AD})$ as functions of $\Delta\omega$ and k with (a) $R_2 = 1.0$, (b) 0.0, and (c) -1.0 when $R_1 = 1.0$. The colored and white regions represent the AD and non-AD regions, respectively. The blue dotted line represents the EP. (d) t_{AD} as a function of k when $R_2 = 1.0$ (black), 0.0 (red), and -1.0 (green) when $\Delta\omega = 4.0$.

We note that there are the same topological structures of eigenvalues near the EPs in coupled limit-cycle oscillators with the parameter space $(\Delta R, \Delta\omega)$ when $k = 2.0$, according to Eq. (7).

C. Numerical results

In order to confirm the role of the EP expected in the previous subsection, we obtain the time series of z_1 and z_2 as k increases. Figure 5 shows the time series of real parts of z_1 and z_2 with different k when $\Delta\omega = 4.0$ and $R_1 = R_2 = 1.0$. The coupling is turned on at $t = 10.0$, i.e., $k = 0.0$ when $t < 10.0$. At $k = 0.5$, neither AD nor 1:1 frequency locking occurs because of small coupling strength. Let us remind that the AD and 1:1 frequency locking occur when the maximal value of Re(λ) in Fig. 3(d) is lower than zero and the pair of Im(λ) in Fig. 3(e) are equal to each other, respectively. At $k = 1.1$, the AD occurs with transient behavior of envelope oscillation but there is no frequency locking on the transient behavior. At $k = 2.0$, the AD occurs without envelope oscillatory transient behavior and the decay is fastest because this is the condition of the EP. The 1:1 frequency locking on the transient behavior is also shown. At $k = 2.4$, the AD occurs without envelope oscillation and there is frequency locking on the transient behavior. The decay is slower than that in the case of $k = 2.0$. At $k = 3.0$, the AD does not occur, but there is frequency locking. In the AD region $(1.0 < k < 2.5)$, the EP is the transition point between decaying *with* and *without* envelope oscillations. Also, in this region, the EP is the transition point for frequency locking. The imaginary parts of eigenvalues relating to the frequencies change two different values into one value via the EP when $R_2 = 1.0$. If $R_1 \neq R_2$, two different frequencies are changed into two close frequencies not an identical frequency and therefore there is no exact frequency locking of transient.

The important role of EP in AD is that the condition of EP guarantees the fastest attracting time to the origin, i.e., the AD state. We investigate the attracting time to the AD state, denoted by t_{AD}. Here, t_{AD} is calculated as follows: If, at time t, the radii of two oscillators first become smaller than c_{AD}, i.e., the criterion for the AD state, and continue to be smaller than c_{AD} for 200 s, then t_{AD} is equal to $t - t_{on}$, where t_{on} is the time when the coupling is turned on. We set $c_{AD} = 0.001$ and $t_{on} = 10.0$. Figures 6(a)–6(c) show $-(1/t_{AD})$, with various R_2 when $R_1 = 1.0$, on the parameter space $(\Delta\omega, k)$. Figure 6(d) shows $-(1/t_{AD})$ as a function of k when $R_1 = 1.0$ and $\Delta\omega = 4.0$ and the local minimum appears more clear when the parameters of system are closer to the EP. Contrary to the expectation from the maximal real parts of eigenvalues in Fig. 3, there are many wrinkled patterns when $R_2 = 1.0$. The wrinkled patterns gradually disappear as R_2 decreases and then there are no patterns when $R_2 = -1.0$. The different t_{on}, which means the different initial conditions, makes the different wrinkled patterns. The wrinkled patterns when $k < \Delta\omega/2$ are caused by the oscillatory transient behavior. However, the reason for the wrinkled patterns when $k > \Delta\omega/2$ is that the transition from fast decay to slow decay occurs when the amplitudes of the oscillators are smaller than our critical value c_{AD} and therefore the patterns disappear if c_{AD} is sufficiently small.

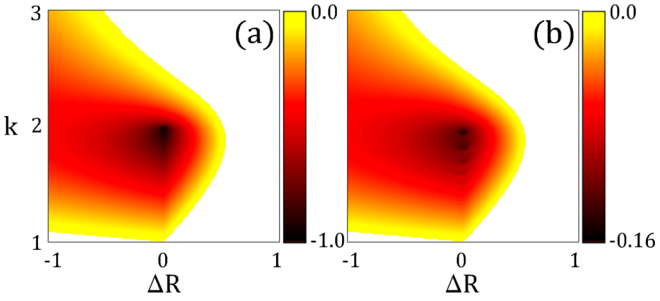

FIG. 7. (Color online) (a) Maximum of real parts of eigenvalues and (b) $-(1/t_{\mathrm{AD}})$ as functions of ΔR and k with $\Delta\omega = 4.0$. The colored and white regions represent the AD and non-AD regions, respectively.

Figure 7 shows the maximal values of real parts of eigenvalues and $-(1/t_{\mathrm{AD}})$ with the parameter space $(\Delta R,k)$ when $\Delta\omega = 4.0$. As shown in Fig. 4, the EP exists at $(\Delta R,k) = (0.0,2.0)$, where the maximal values of real parts of eigenvalues are local minimum, as shown in Fig. 7(a). t_{AD} are also local minimum at the EP. In Fig. 7(b), the wrinkled patterns exist at $\Delta R = 0.0$ but they disappear as ΔR deviates from 0.0. In principle, for the long-time behavior, the oscillation behavior, such as underdamped case, exists only on the line, $\Delta R = 0$ and $k < \Delta\omega/2$, because the real parts of two eigenvalues are the same on the line in the parameter space $(\Delta R,k)$. Different real parts of the two eigenvalues mean the system has two different decay rates and therefore only one frequency is dominant for a long-time behavior. It is noted that the EP is not a local minimal point on the parameter space $(\Delta\omega,k)$ because the EP forms the lines as shown in Figs. 3(a) and 6(a). That is, the maximal values of the real parts of the eigenvalues decrease as the $\Delta\omega$ increases on the EP line, $k = \Delta\omega/2$.

IV. SUMMARY

We have studied the exceptional point in dynamical systems and investigated the role of the exceptional point in the transient behaviors of amplitude death in coupled limit-cycle oscillators. The exceptional point is associated with a critical point of frequency locking as well as the transition of the envelope oscillation, which also gives the fastest decay to the amplitude death in coupled limit-cycle oscillators. In addition, for other examples (two Van der Pol oscillators interacting through mean-field diffusive coupling, and a coupled system consisting of the Rössler and a linear oscillator), we have obtained the largest decay rates and transition behaviors at the exceptional point (not shown here). As a result, the transient behaviors related to the exceptional point appear commonly for the coupled dissipative dynamical systems, independent of the specific properties of systems. We expect the exceptional point is important in the study of various disciplines, such as nonequilibrium statistical mechanics [35] and transient chaos [36,37], because the exceptional point is not related to the stationary states but to the transient behaviors.

ACKNOWLEDGMENTS

This research was supported by Basic Science Research Program through the National Research Foundation of Korea (NRF) funded by the Ministry of Education (No. 2012R1A1A4A01013955 and No. 2013R1A1A2011438), and National Institute for Mathematical Sciences (NIMS) funded by the Ministry of Science, ICT & Future Planning (A21501-3; B21501).

[1] T. Kato, *Perturbation Theory of Linear Operators* (Springer, Berlin, 1996).
[2] W. D. Heiss, J. Phys. A **45**, 444016 (2012), and references therein.
[3] W. D. Heiss, Eur. Phys. J. D **7**, 1 (1999).
[4] O. Latinne, N. J. Kylstra, M. Dörr, J. Purvis, M. Terao-Dunseath, C. J. Joachain, P. G. Burke, and C. J. Noble, Phys. Rev. Lett. **74**, 46 (1995).
[5] H. Cartarius, J. Main, and G. Wunner, Phys. Rev. Lett. **99**, 173003 (2007).
[6] C. Dembowski, H.-D. Gräf, H. L. Harney, A. Heine, W. D. Heiss, H. Rehfeld, and A. Richter, Phys. Rev. Lett. **86**, 787 (2001).
[7] C. Dembowski, B. Dietz, H.-D. Gräf, H. L. Harney, A. Heine, W. D. Heiss, and A. Richter, Phys. Rev. Lett. **90**, 034101 (2003).
[8] S.-B. Lee, J. Yang, S. Moon, S.-Y. Lee, J.-B. Shim, S. W. Kim, J.-H. Lee, and K. An, Phys. Rev. Lett. **103**, 134101 (2009).
[9] C. M. Bender and S. Boettcher, Phys. Rev. Lett. **80**, 5243 (1998).
[10] S. Klaiman, U. Günther, and N. Moiseyev, Phys. Rev. Lett. **101**, 080402 (2008).
[11] C. E. Rueter, K. G. Makris, R. El-Ganainy, D. N. Christodoulides, M. Segev, and D. Kip, Nat. Phys. **6**, 192 (2010).
[12] W. D. Heiss, J. Phys. A **37**, 2455 (2004).
[13] T. Stehmann, W. D. Heiss, and F. G. Scholtz, J. Phys. A **37**, 7813 (2004).
[14] G. Saxena, A. Prasad, and R. Ramaswamy, Phys. Rep. **521**, 205 (2012), and references therein.
[15] K. B. Eli, J. Phys. Chem. **88**, 3616 (1984).
[16] R. E. Mirollo and S. Strogatz, J. Stat. Phys. **60**, 245 (1990).
[17] G. B. Ermentrout, Physica D **41**, 219 (1990).
[18] D. G. Aronson, G. B. Ermentrout, and N. Kopell, Physica D **41**, 403 (1990).
[19] D. V. R. Reddy, A. Sen, and G. L. Johnston, Phys. Rev. Lett. **80**, 5109 (1998).
[20] D. V. Ramana Reddy, A. Sen, and G. L. Johnston, Physica D **129**, 15 (1999).
[21] D. V. Ramana Reddy, A. Sen, and G. L. Johnston, Phys. Rev. Lett. **85**, 3381 (2000).
[22] D. V. Ramana Reddy, A. Sen, and G. L. Johnston, Physica D **144**, 335 (2000).
[23] W. Zou, D. V. Senthilkumar, Y. Tang, Y. Wu, J. Lu, and J. Kurths, Phys. Rev. E **88**, 032916 (2013).
[24] R. Karnatak, N. Punetha, A. Prasad, and R. Ramaswamy, Phys. Rev. E **82**, 046219 (2010).
[25] K. Konishi, Phys. Rev. E **68**, 067202 (2003).
[26] A. Prasad, Y. C. Lai, A. Gavrielides, and V. Kovanis, Phys. Lett. A **318**, 71 (2003).

[27] A. Prasad, M. Dhamala, B. M. Adhikari, and R. Ramaswamy, Phys. Rev. E **81**, 027201 (2010).
[28] F. M. Atay, Physica D **183**, 1 (2003).
[29] R. Dodla, A. Sen, and G. L. Johnston, Phys. Rev. E **69**, 056217 (2004).
[30] K. Konishi, Phys. Rev. E **70**, 066201 (2004).
[31] Z. Hou and H. Xin, Phys. Rev. E **68**, 055103 (2003).
[32] W. Liu, X. Wang, S. Guan, and C. H. Lai, New J. Phys. **11**, 093016 (2009).
[33] A. Koseska, E. Volkov, and J. Kurths, Phys. Rep. **531**, 173 (2013).
[34] M. Kantner, E. Schöll, and S. Yanchuk, Sci. Rep. **5**, 8522 (2015).
[35] R. Zwanzig, *Nonequilibrium Statistical Mechanics* (Oxford University Press, Oxford, U.K., 2001).
[36] Y.-C. Lai and T. Tél, *Transient Chaos: Complex Dynamics on Finite-Time Scales* (Springer, New York, 2013).
[37] A. E. Motter, M. Gruiz, G. Károlyi, and T. Tél, Phys. Rev. Lett. **111**, 194101 (2013).